



SUBJECT AREAS:

SYNAPTIC
TRANSMISSION

DEVELOPMENT

PLASTICITY

CELLULAR NEUROSCIENCE

Developmental regulation of CB1-mediated spike-time dependent depression at immature mossy fiber-CA3 synapses

Maddalena D. Caiati¹, Sudhir Sivakumaran^{1,4}, Frederic Lanore², Christophe Mulle², Elodie Richard³, Dany Verrier³, Giovanni Marsicano³, Richard Miles⁴ & Enrico Cherubini¹

Received

19 December 2011

Accepted

30 January 2012

Published

24 February 2012

Correspondence and requests for materials should be addressed to E.C. (cher@sissa.it)¹Neurobiology Dept. and Italian Institute of Technology Unit, International School for Advanced Studies, Trieste, Italy, ²Interdisciplinary Institute for Neuroscience, CNRS UMR 5297, Bordeaux, France, ³INSERM U862, Bordeaux, France, ⁴INSERM UMRS975, Paris, France.

Early in postnatal life, mossy fibres (MF), the axons of granule cells in the dentate gyrus, release GABA which is depolarizing and excitatory. Synaptic currents undergo spike-time dependent long-term depression (STD-LTD) regardless of the temporal order of stimulation (*pre versus post* and *viceversa*). Here we show that at P3 but not at P21, STD-LTD, induced by negative pairing, is mediated by endocannabinoids mobilized from the postsynaptic cell during spiking-induced membrane depolarization. By diffusing backward, endocannabinoids activate cannabinoid type-1 (CB1) receptors probably expressed on MF. Thus, STD-LTD was prevented by CB1 receptor antagonists and was absent in *CB1-KO* mice. Consistent with these data, *in situ* hybridization experiments revealed detectable level of CB1 mRNA in the granule cell layer at P3 but not at P21. These results indicate that CB1 receptors are transiently expressed on immature MF terminals where they counteract the enhanced neuronal excitability induced by the excitatory action of GABA.

The axons of granule cells in the dentate gyrus, the mossy fibres (MFs) provide most of the excitatory drive to CA3 principal cells and GABAergic interneurons of the hilus and stratum lucidum¹. Early in postnatal development MF release GABA which exerts a depolarizing and excitatory action on target neurons^{2,3}. Immature MFs are endowed with kainate receptors (KARs) and GABA_B receptors, whose activation reduces GABA release leading in some cases to synapse silencing^{4,5}.

Immature MF-CA3 synapses undergo activity-dependent modifications of synaptic efficacy which are crucial for learning and memory processes and for the refinement of neuronal circuits. Thus, calcium transients associated with giant depolarizing potentials or GDPs, a hallmark of developmental networks, act as coincident detectors for enhancing synaptic efficacy in an associative manner⁶. In addition, immature MF-CA3 synapses exhibit spike time-dependent long-term depression (STD-LTD)⁷, an associative form of learning crucial for information coding. STD-LTD occurs regardless of the temporal order of stimulation (*pre versus post* and *viceversa*). However, STD-LTD induced by positive pairing (*pre before post*) can be switched to STD-long-term potentiation (LTP) by blocking presynaptic GluK1-containing KARs with selective antagonists, indicating that KARs activated by 'ambient' glutamate control the direction of STD-LTD⁵. However, in the presence of KAR antagonists, negative pairing (*postsynaptic spiking before MF stimulation*) still induces LTD, suggesting that KARs are not involved in this form of synaptic plasticity. Studies from several brain structures have shown that STD-LTD is controlled by endocannabinoids, which activate presynaptic CB1 receptors *via* retrograde signalling and suppress neurotransmitter release at both excitatory and inhibitory synapses^{8,9}. Here we show that, at immature MF-CA3 synapses, the persistent weakening of synaptic strength induced by correlating postsynaptic spiking with presynaptic MF activation involves CB1 signalling. Thus, STD-LTD was prevented by selective CB1 receptor antagonists and was absent in *CB1-KO* mice. In addition, CB1-mediated STD-LTD could not be induced at late developmental stages when MF release glutamate on their targets.



Results

Single MF-evoked GABA_A-mediated postsynaptic currents (GPSCs) were recorded at -60 mV from P3–P6 CA3 pyramidal cells in the presence of DNQX (50 μ M) and D-AP5 (50 μ M) to block AMPA/kainate and NMDA receptors, respectively. Negative pairing (post 50 ms before pre; Fig. 1A and B) induced in 28/44 neurons (64%) a persistent depression of MF-GPSCs (see also⁷). Thirty minutes after pairing, the mean peak amplitude of GPSCs (successes plus failures) obtained in all neurons tested (exhibiting or not LTD) was 64.4 ± 3.3 % of pre-pairing values ($n=44$; $p<0.001$; paired t -test; Fig. 1C and D). In cells exhibiting LTD ($n=28$), synaptic depression was associated with a decrease of successes rate (from 0.63 ± 0.05 to 0.39 ± 0.04 , before and after pairing, respectively; $n=28$; $p<0.001$; paired t -test), a decrease in the inverse square value of CV (from 2.98 ± 0.68 to 1.12 ± 0.25 ; $n=28$; $p<0.001$; paired t -test) and an increase in PPR (from 1.09 ± 0.21 to 1.98 ± 0.49 ; $n=12$; $p<0.001$; paired t -test; Fig. 1E), indicating a reduction in the probability of GABA release. To further assess whether STD-LTD results from a reduced GABA release from MF terminals, we analyzed the coefficient of variation

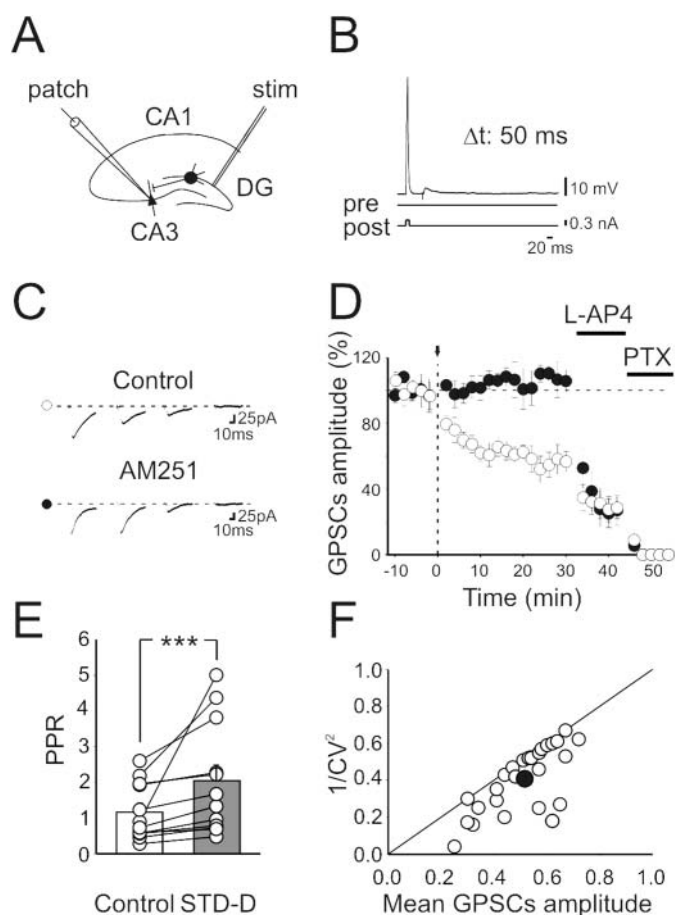


Figure 1 | STD-LTD requires the activation of CB1 receptors. (A) Schematic representation of the experimental design. (B) The stimulation of granule cells in the dentate gyrus followed the postsynaptic spike by 50 ms. (C) MF-GPSCs evoked before, after pairing, after addition of L-AP4 or L-AP4 plus picrotoxin (PTX), in the absence (Control) or in the presence of AM251 (each trace is the average of 30–60 trials including failures). (D) Mean GPSCs amplitude (before and after pairing, arrows at time 0) is plotted against time. Open circles: control ($n=44$); closed circles: in the presence of AM251 ($n=12$); vertical bars are SEM. (E) Paired-pulse ratio measured before (Control) and after pairing in neurons exhibiting LTD (grey STD-D; $n=12$). $***p<0.001$. (F) Plot of $1/CV^2$ versus GPSCs amplitude measured after LTD induction and normalized to respective controls. The closed circle indicate the mean (SEM is within the symbols).

before and 30 min after the induction of pairing. Normalized plots of $1/CV^2$ versus mean yielded points lying on or below the diagonal, further suggesting that the locus of depression is presynaptic¹⁰ (Fig. 1D). Postsynaptic spiking (10 spikes at 0.1 Hz) in the absence of presynaptic stimulation did not modify MF-GPSCs.

The induction of STD-LTD may require postsynaptic calcium influx through spike-induced membrane depolarization. We tested this possibility by loading the postsynaptic cell with the calcium chelator BAPTA (20 mM). BAPTA prevented the induction of STD-LTD (mean peak amplitude of GPSCs: $95.6 \pm 5\%$ of controls, $n=13$; $p=0.7$; paired t -test; Fig. 2), indicating that this form of synaptic plasticity is due to an increased calcium level in the postsynaptic cell. Calcium influx occurs *via* voltage-dependent calcium channels (VDCC) since STD-LTD was completely blocked by nifedipine (10 μ M) a VDCC blocker (after pairing, the mean peak amplitude of GPSCs was $94.9 \pm 3.1\%$ of controls; $n=8$; $p=0.1$; paired t -test; Fig. 2).

Our data demonstrate a postsynaptic induction of STD-LTD, but a presynaptic expression as suggested by the increase in PPR and the decrease in CV^{-2} of MF-GPSCs. The postsynaptic cell must then provide a paracrine retrograde signal to the presynaptic neuron. Possible candidates are endocannabinoids (eCBs), mobilized from principal neurons and known to mediate several forms of retrograde short- and long-term presynaptic depression⁹. Once released, eCBs diffuse to activate CB1 receptors localized on presynaptic neurons and inhibit transmitter release.

To determine whether STD-LTD was CB1-dependent, we applied the selective CB1 antagonist AM251. AM251 (5 μ M) *per se* did not modify synaptic activity (see Supplementary Fig. S1 online). However, this compound fully prevented STD-LTD in all cells tested, indicating the involvement of CB1 receptors. In the presence of AM251, the peak amplitude of MF-GPSCs was $97.4 \pm 2.7\%$ of controls ($n=12$; $p=0.37$; paired t -test; Fig. 1C and D). Failure of inducing LTD in a minority of cases (36%) suggests that either endocannabinoids released from principal cells failed to reach MF terminals or that some MF terminals do not express CB1 receptors. In agreement with other studies on different brain structures^{11–13}, application of AM251 20 min after the induction of STD-LTD did not modify the amplitude of synaptic responses indicating that the activation of CB1 receptors is necessary for the induction, but not for the maintenance of STD-LTD (see Supplementary Fig. S1 online).

To further assess the involvement of CB1 receptors in STD-LTD, the pairing procedure was applied to CA3 principal cells in hippocampal slices obtained from P3–P6 *CB1*-KO mice and WT littermates. As in rats, negative pairing induced a significant and

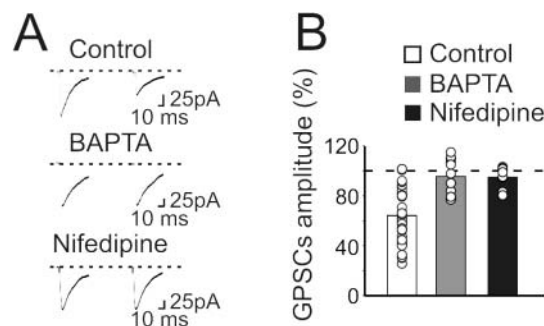


Figure 2 | Pairing-induced LTD requires a calcium influx in the postsynaptic cell *via* voltage-dependent calcium channels. (A) Averaged traces of MF-GPSC (30 to 60 trials including failures) evoked before and 20 min after pairing in control, in neurons loaded with intracellular BAPTA (20 mM) or exposed to nifedipine (10 μ M). (B) Pairing-induced changes in the mean amplitude of MF-GPSCs in control ($n=44$), in cells loaded with BAPTA ($n=13$) or exposed to nifedipine (black column; $n=8$).



persistent depression of MF-GPSCs. Pooled data from animals exhibiting ($n=9$; 69 % of cases) or not ($n=4$) LTD are reported in Fig. 3. After pairing the mean GPSC amplitude was $57.8 \pm 4.5\%$ of control values ($p=0.003$; paired t -test; Fig. 3). In cells exhibiting LTD, synaptic depression was associated with a decrease in success rate (from 0.67 ± 0.07 to 0.33 ± 0.06 , before and after pairing, respectively; $n=9$; $p<0.001$; paired t -test) and a decrease in the inverse square value of CV (from 3.5 ± 0.58 to 1.6 ± 0.3 ; $n=9$; $p=0.003$; paired t -test). In contrast, in *CB1*-KO mice the pairing protocol did not cause STD-LTD (mean peak amplitude of GPSCs $101.7 \pm 4.7\%$ of controls; $n=10$; $p=0.3$; paired t -test; Fig. 3), providing further evidence that CB1 receptors are involved in STD-LTD.

If STD-LTD is mediated by CB1 receptors, the possibility to block this form of synaptic plasticity with BAPTA and nifedipine indicates that secretion of eCBs from principal cells is triggered by the elevation of intracellular calcium *via* VDCC. However, signalling *via* group I mGluR might also contribute to intracellular calcium rise *via* PLC, as described for some forms of eCBs-dependent synaptic plasticity^{12,14}. Therefore, we tested whether the selective mGluR1 and mGluR5 antagonists LY 367385 and MPEP, respectively were able to prevent STD-LTD. Bath application of LY 367385 (100 μ M) and MPEP (5 μ M), either alone or in combination, failed to affect STD-LTD. In the presence of LY 367385 plus MPEP, the peak amplitude of MF-GPSCs reached $65 \pm 7.3\%$ of control values ($n=9$; $p=0.88$; one-way ANOVA; see (see Supplementary Fig. S2 online) indicating that group I mGluR are not involved. Furthermore, STD-LTD did not result from an indirect modulation of eCBs by receptors that depress transmitter release such as GABA_B, nicotine and muscarinic acetylcholine receptors, purinergic P2Y and adenosine receptors since the pairing procedure still induced STD-LTD in the presence of the respective antagonists (see Supplementary Fig. S2 online).

Anandamide and 2-arachidonylglycerol (2-AG) are well studied endogenous ligands at cannabinoid receptors⁸. In order to identify which of these two molecules is involved in STD-LTD, the postsynaptic cell was loaded with THL, an inhibitor of diacylglycerol lipase activity^{15,16}. THL did not affect STD-LTD: pairing postsynaptic spiking with presynaptic MF stimulation reduced the peak amplitude of MF-GPSCs to $59 \pm 8\%$ as in the absence of the drug ($n=9$; $p=0.03$; paired t -test; see Supplementary Fig. S3 online). The depressant effect was not significantly different from that obtained in the absence of THL ($p=0.76$; one-way ANOVA). THL failed to block STD-LTD also when it was applied in the bath at the concentration of 10 μ M; 20 min after pairing, the peak amplitude of GPSCs was $51.7 \pm 0.12\%$ of controls; $n=5$; $p<0.05$; paired t -test; data not shown). These data suggest that 2-AG is not involved in STD-LTD.

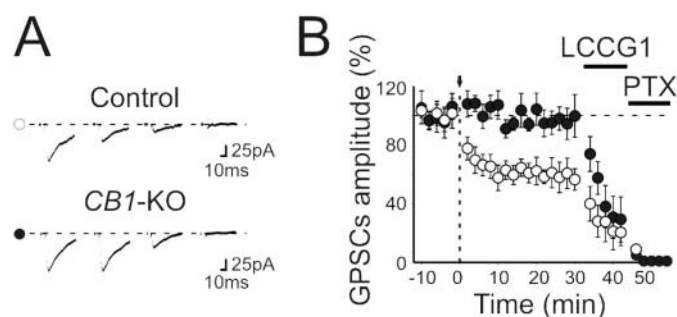


Figure 3 | Lack of STD-LTD in *CB1*-KO mice. (A) MF-GPSCs evoked before, after pairing, after addition of LCCG1 or LCCG1 plus PTX, in WT mice (open circle, Control) or in *CB1*-KO mice (closed circle). (B) Summary plot of mean MF-GPSCs amplitude (before and after pairing, arrows at time 0) versus time in WT (open circles; $n=9$) or in *CB1*^{-/-} mice (closed circles; $n=10$). Data from WT animals are pooled between those exhibiting ($n=9$) or not ($n=4$) LTD.

To further investigate the endogenous eCB ligand involved in STD-LTD, we next used drugs that alter endocannabinoids degradation. In the brain, anandamide is metabolized by the fatty acid amide hydrolase (FAAH)¹⁷. Inhibition of FAAH with URB597 (1 μ M) did not modify basic synaptic transmission or change the magnitude of STD-LTD. In the presence of URB597, the pairing procedure reduced the peak amplitude of MF-GPSCs to $62 \pm 5\%$ of controls ($n=7$; $p<0.05$; paired t -test). However, URB597 lengthened up to 100 ms the time window (between postsynaptic spiking and presynaptic stimulation) necessary for the induction of STD-LTD (Fig. 4; see also¹²). Pairing with a delay of 100 ms reduced the peak amplitude of GPSCs to $58 \pm 7\%$ of controls ($n=9$; $p=0.03$; paired t -test). A further prolongation of the delay between post and presynaptic stimulation to 200 ms failed to induce STD-LTD ($99.7 \pm 1.2\%$ of control; $n=5$; $p=0.5$; paired t -test). Similar data were obtained with AM404¹⁷ (10 μ M) which inhibits the carrier responsible for anandamide internalization and degradation (Fig. 4). In contrast, JZL 184 (1 μ M), which increases the levels of 2-AG by blocking monoacylglycerol lipase, the enzyme responsible for 2AG degradation, did not alter the time window for LTD induction (Fig. 4). These data show that limiting the uptake or the degradation of anandamide prolongs the time window for the induction of STD-LTD, whereas inhibition of synthesis or degradation of 2-AG does not alter this form of synaptic plasticity. Therefore, these results suggest that anandamide is the main mediator of STD-LTD.

If STD-LTD is mediated by CB1 receptors, CB1 agonists should be able to occlude this form of synaptic plasticity. Overall, in 17 neurons, the CB1 receptor agonist WIN 55,212-2 (2 μ M) reduced the peak amplitude of GPSCs to $69 \pm 5\%$ of controls ($p=0.003$; Fig. 5D). These data include also 5 neurons in which WIN 55,212-2 was ineffective. In 12/17 neurons (70.5 %) WIN 55,212-2 reduced the peak amplitude of GPSCs to $57.1 \pm 3.4\%$ of controls ($p<0.001$; paired t -test; Fig. 5A and C). WIN 55,212-2 depressed MF-GPSCs by reducing the probability of GABA release from MF terminals since it decreased the inverse square of CV and increased the PPR, which is inversely correlated with release probability¹⁸ (see Supplementary Fig. S4 online). Importantly, when the pairing protocol was applied after WIN 55,212-2, no further depression of GPSCs was obtained, indicating occlusion (Fig. 5A and C). However, these experiments should be interpreted with caution in view of the reported effects of WIN 55,212-2 on presynaptic calcium channels¹⁹. Furthermore, STD-LTD induction occluded all effects of WIN 55,212-2 (Fig. 5B and C). Similarly, anandamide (AEA, 30 μ M) reduced in 9/13 neurons GPSCs amplitude. The depression of GPSCs amplitude obtained in all cells tested (included those not affected by AEA) was $69.5 \pm 5.6\%$ of controls ($n=13$; $p=0.01$; Fig. 5D). In 69.2% of neurons AEA depressed the peak amplitude of GPSCs to $43.3 \pm 3\%$ of controls ($n=9$; $p=0.004$), an effect that was blocked by AM251 ($n=10$; $p=0.31$; paired t -test; Fig. 5D), further indicating that anandamide acts on CB1 receptors. Occlusion was also found between the depressant effects of AEA on GPSCs and STD-LTD ($n=5$; data not shown). As expected for eCB-induced synaptic depression, a partial recovery of GPSCs amplitude towards pre-drug values (to $76.7 \pm 9.4\%$ of control; $n=5$) was obtained when the CB1 antagonist AM251 was applied 15 minutes after WIN (data not shown).

In the developing hippocampus, CB1-dependent heterosynaptic LTD observed in the CA1 region is associated with a decrease in presynaptic fibres excitability²⁰. We asked whether eCBs may affect axonal excitability, by recording antidromic spikes from single granule cells held at -70 mV in the absence or in the presence of the CB1 receptor agonist WIN 55,212-2. MFs were stimulated *via* an electrode positioned in *stratum lucidum* and the stimulus strength was adjusted to evoke antidromic spikes in $> 60\%$ of trials. WIN 55,212-2 (2 μ M) reduced the probability of evoking antidromic spikes to $54.6 \pm 5.7\%$ of controls ($n=7$; $p<0.001$; paired t -test; Fig. 6), indicating that

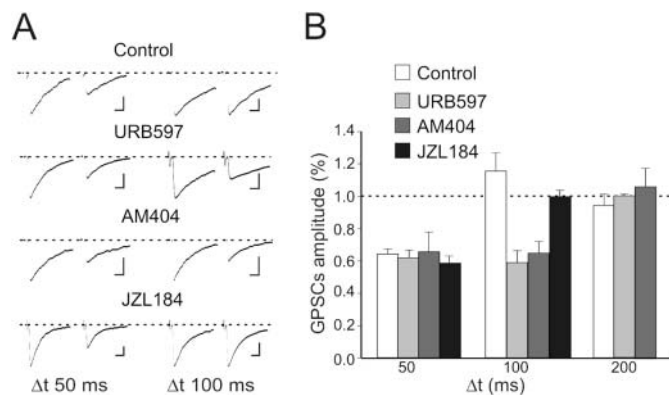


Figure 4 | Blocking anandamide degradation lengthens the time window for STD-LTD induction. (A) MF-GPSCs obtained in control, in the presence of the FAAH inhibitor URB597 (1 μ M), of the carrier inhibitor responsible for anandamide internalization and degradation AM404 (10 μ M) and of the monoacylglycerol lipase inhibitor JZL 184 (1 μ M), the enzyme responsible for 2AG degradation, at Δt of 50 and 100 ms. Calibration: 10 ms and 50 pA. (B) Summary plot of MF-GPSCs obtained in control ($n = 44, 5$ and 5), in the presence of URB597 ($n = 7, 9$ and 5), AM404 ($n = 5, 7$ and 5) or JZL 184 ($n = 6, 15$) at different time windows (Δt) between postsynaptic spiking and presynaptic stimulation. Note that while URB597 and AM404 prolonged the time windows for inducing STD-LTD, JZL 184 did not.

activation of CB1 receptors probably located on MF terminals reduces MF excitability. This effect was blocked by AM 251 (Fig. 6).

It is well known that CB1 receptors are not expressed on juvenile glutamatergic MF terminals^{16,21,22}. Therefore, in the following experiments we tested whether the same pairing protocol used in neonates can induce CB1-dependent STD-LTD at MF-evoked glutamatergic excitatory postsynaptic currents (EPSCs) in CA3 principal cells of P19–P25 old animals. These experiments were routinely performed in the presence of picrotoxin (100 μ M) to block GABA_A receptors. Consistent with their MF origin, EPSCs were highly sensitive to group II mGluR agonist DCG-IV²³. At the concentration of 4

μ M this compound induced a $75.8 \pm 2.1\%$ reduction in the peak amplitude of EPSCs (Fig. 7). As shown in Fig. 7, negative pairing (post before pre) failed to modify synaptic strength in all neurons tested ($n = 19$; from 6 rats). After pairing the EPSCs amplitude was $104 \pm 7\%$ of controls ($p = 0.84$; paired t -test).

Our electrophysiological data support the assumption that CB1 receptors are only transiently expressed on MF terminals in the immediate postnatal period. To validate this hypothesis *in situ* hybridization (ISH) experiments were performed from granule cells at P3 and P21 to assess whether CB1 mRNA expression follows a similar developmental profile. In the hippocampus of adult mice,

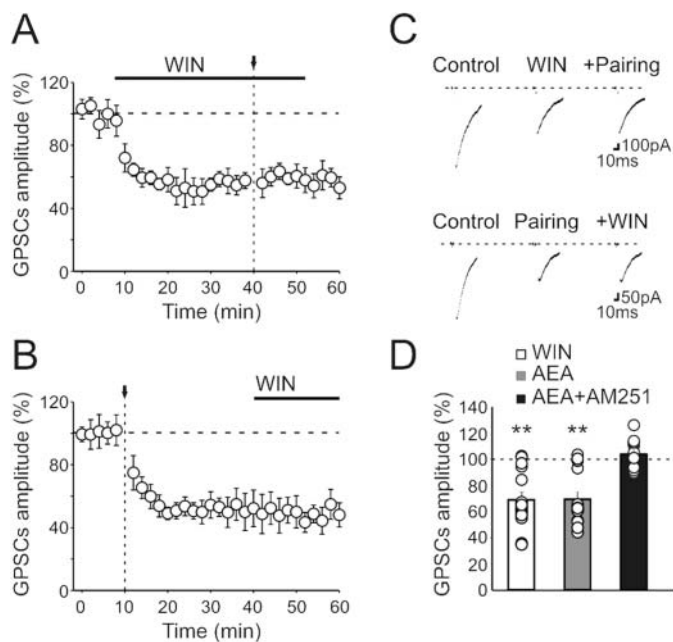


Figure 5 | CB1 receptor agonists reduce the amplitude of MF-GPSCs. (A) The depressant effect of WIN 55,212-2 (2 μ M, bar) on MF-GPSCs was occluded by subsequent pairing (arrow, $n = 12$). (B) When WIN 55,212-2 (bar) was applied after pairing (arrow) it did not affect MF-GPSCs ($n = 8$). (C) Individual samples (average of 30 to 60 responses including failures) from A and B respectively. (D) Mean MF-GPSCs amplitude obtained in all cells tested after application of WIN 55,212-2 ($n = 17$), AEA ($n = 13$) or AEA plus AM351 ($n = 10$). Note that AM251 completely antagonized the effects of AEA on MF-GPSCs. $**p \leq 0.01$.

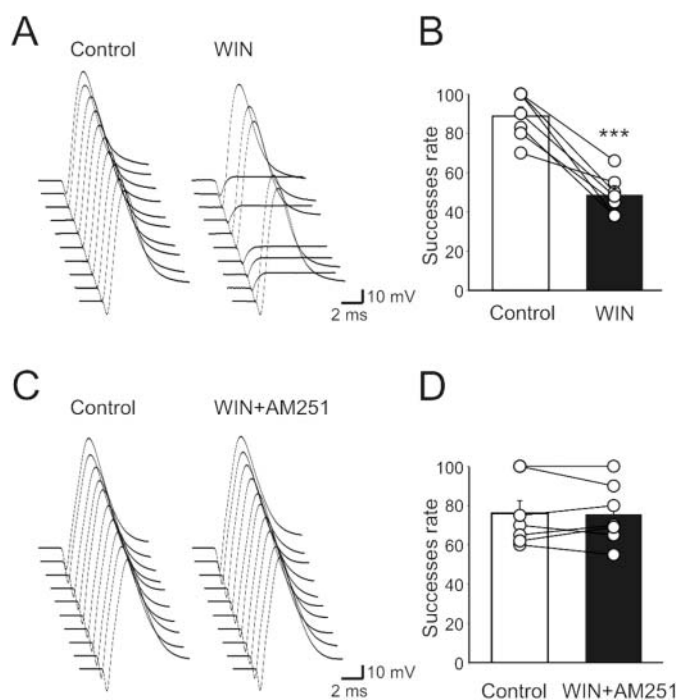


Figure 6 | Activation of CB1 receptors with WIN 55,212-2 reduces MF excitability. (A) Antidromic spikes evoked in granule cells upon stimulation of MF in stratum lucidum before and during bath application of WIN 55,212-2 (note that in this particular case the stimulus strength was set to obtain 100% of successes). (B) Summary plot for the examples shown in A ($n = 7$). C–D As in A–B but in the presence of AM251 ($n = 7$); $***p < 0.001$.



CB1 mRNA is detected at very high levels in GABAergic interneurons and at low levels in CA1 and CA3 pyramidal neurons but not in granule cells²¹. Interestingly, in the present experiments at P3 granule cells displayed low, but detectable levels of CB1 mRNA (Fig. 8 A), which were clearly above background levels as determined in sections from *CB1*-KO mice (Fig. 8 A). In line with electrophysiological data however, this expression was lost at P21 mice (Fig. 8 B). Thus, granule cells transiently express CB1 mRNA only at early stages of postnatal development.

Discussion

Both pharmacological (selective CB1 antagonists) and mouse genetic (*CB1*-KO mice) data clearly demonstrate that STD-LTD induced by negative pairing is mediated by activation of $G_{i/o}$ -coupled CB1 receptors at immature MF-CA3 synapses. Endocannabinoids are phospholipids that are synthesised and released from brain cells to regulate neuronal activity and synaptic plasticity^{8,17}. Our results show the induction of STD-LTD is postsynaptic, triggered by calcium influx *via* voltage-dependent calcium channels activated by spiking-induced membrane depolarization. Thus, the calcium chelator BAPTA may interfere with eCBs production to abolish LTD^{24,25}. In agreement with our data, previous studies have demonstrated that, the developmentally regulated expression of eCB-dependent long-term reduction of glutamate release in different brain regions relies on postsynaptic mechanisms including calcium rise *via* VDCC^{26,27}. Our results exclude the contribution of many G protein-coupled receptors known to stimulate eCB production in other contexts⁹ since STD-LTD was preserved in the presence of specific receptor antagonists.

Anandamide and 2-AG are endocannabinoids known to regulate synaptic transmission mainly through presynaptic CB1 receptors¹⁷. While 2-AG seems to be rather specific for CB1 receptors, anandamide binds to both CB1 and vanilloid type 1 (TRPV1) receptors²⁸. At inhibitory synapses, 2-AG has been proposed to mediate different forms of long- and short-term synaptic plasticity, which are affected by specific inhibitors of synthesis, uptake or degradation of this endocannabinoid^{8,9}. However, the other major endocannabinoid has also been proposed to mediate different forms of synaptic plasticity, such as LTD at excitatory synapses in the basal ganglia²⁷ or LTD at inhibitory synapses in the amygdala²⁹. Our data strongly suggest that 2-AG is not involved in STD-LTD, since blockade of 2AG synthesis (by intracellular and bath-applied THL) or degradation (by JZL 184) did not affect pairing-induced synaptic depression. Several lines of evidence support instead the involvement of anandamide in

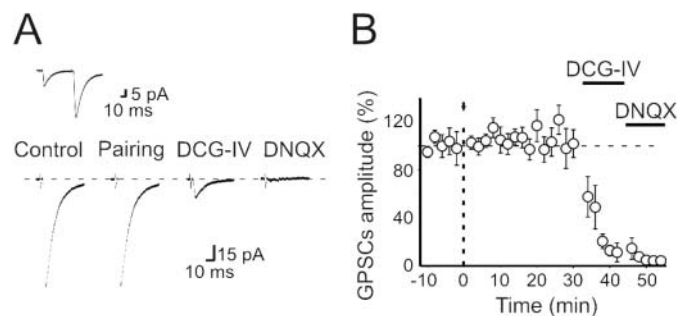


Figure 7 | Lack of CB1-mediated STD-LTD in hippocampal slices obtained from P19–P25 old rats. (A) Glutamatergic MF-EPSCs evoked in the presence of picrotoxin (100 μ M) before (Control), after pairing, after addition of DCG-IV or DCG-IV plus DNQX. The inset above the traces shows paired pulse facilitation of MF-EPSCs. (B) Mean amplitude of MF-EPSCs before and after pairing (arrows at time 0) *versus* time ($n = 19$). Note that pairing did not affect synaptic responses. These were strongly reduced by DCG-IV and blocked by DNQX.

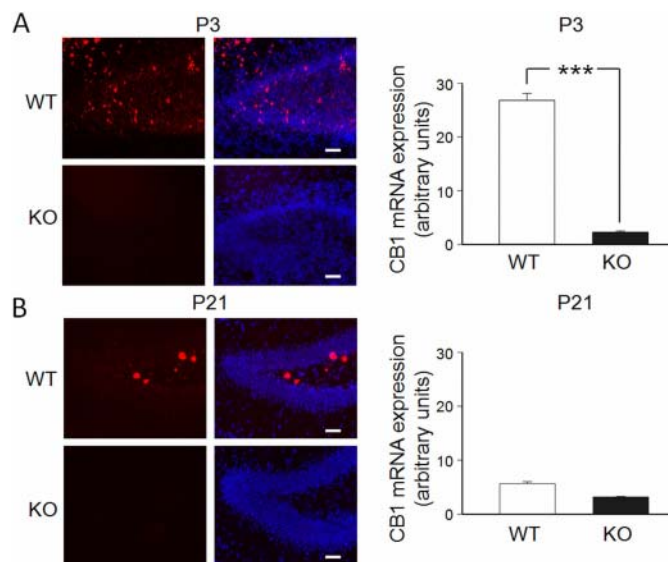


Figure 8 | Developmentally-regulated expression of CB1 mRNA in the granule cell layer of the dentate gyrus. (A) and (B) On the left, photomicrographs representing CB1 mRNA staining (red) alone or together with DAPI nuclear counterstaining (blue) in the dentate gyrus of WT and *CB1*-KO mice at P3 (A) and at P21 (B) animals. Cal. bar: 20 μ m. On the right, Each column represents the averaged value of CB1 mRNA expression obtained in 4–8 sections corresponding to dorsal DG of WT or *CB1*-KO mice at P3 and at P21 (2 mice per group; see methods). *** $p < 0.001$.

STD-LTD. Thus, inhibiting anandamide transport with AM404³⁰ or its degradation with URB597^{31,32} lengthened the time window for LTD, suggesting that anandamide is the endogenous ligand released by principal cells. Anandamide was acting on CB1 and not TRPV1 receptors since the effects of this molecule on GPSCs were antagonized by the CB1 receptor antagonist AM251 and the pairing protocol failed to induce STD-LTD in animals lacking CB1 receptors. Variation in the rate of eCBs production or inactivation may account for differences in the temporal window for LTD observed at different synapses^{12,28}. While STD-LTD is induced postsynaptically, its expression seems to be presynaptic judged by pairing-induced changes in the number of successes, $1/CV^2$ and PPR. In particular, analysis of the CV of synaptic responses indicates a presynaptic expression site presumably associated with a reduced GABA release¹⁰. The suppression of STD-LTD by CB1 receptor antagonists points to a locus of expression coinciding with CB1 receptors. Possibly, eCBs are produced by postsynaptic neurons and diffuse retrogradely to activate CB1 receptors on MF terminals. Further evidence that CB1 receptors are involved in STD-LTD is given by data showing that the depressant effects of WIN 55,212-2 or AEA on synaptic currents were occluded by STD-LTD, indicating that both STD-LTD and WIN 55,212-2 act on the same targets. As for STD-LTD, the locus of WIN 55,212-2 and AEA action was clearly presynaptic as suggested by the decrease in CV^2 values and the increase in PPR. WIN 55,212-2 may depress GPSCs amplitude by reducing MF excitability, since it decreased the probability of evoking antidromic spikes. Changes in fibre excitability due to potassium channel activation have been implicated in eCB-mediated heterosynaptic depression at Schaffer collateral-CA1 synapses in developing hippocampus²⁰. Whatever the mechanisms, our work clearly suggests that, early in postnatal life, CB1 receptors are expressed on the axons of cells projecting from the granule cell layer to stratum lucidum.

Previous reports failed to show the presence of CB1 receptors on adult glutamatergic MF terminals^{16,22} or CB1 mRNA in adult granule



cells²¹ and in agreement with these findings we failed to induce CB1-mediated STD-LTD at glutamatergic MF-CA3 synapses in the hippocampus of juvenile animals, using the same protocol of neonates. However, it is worth noting that a NMDA-dependent form of STD-LTD can be induced at these synapses using a different stimulating paradigm²³.

Consistent with the involvement of endocannabinoid signalling at immature MF-CA3 synapses, *in situ* hybridization experiments revealed clearly detectable levels of CB1 mRNA in the granule cell layer of the hippocampus of P3 old animals. In older animals instead, the expression of CB1 mRNA was drastically reduced (if not absent; see also Ref 21), suggesting that in this area CB1 expression is developmentally regulated. Although we cannot exclude that, at P3, cells more strongly labelled belongs to GABAergic interneurons, their involvement in STD-LTD seems unlikely since all neurons tested were severely depressed by L-AP4 or LCCG1 while GABAergic interneurons are usually not sensitive to mGluR agonists^{23,33}. In addition, the reduced probability of evoking antidromic spikes in granule cells exposed to WIN 55,212-2, a selective CB1 agonist, suggests that CB1 receptors are expressed on cells projecting from the granule cell layer to the stratum lucidum. Whether stimulated axons originate from granule cells or progenitors expressing a GABAergic phenotype is still a matter of debate^{23,34}. Alternatively, we cannot exclude the possibility that anandamide binds to CB1 receptors present on different cell types (i.e. astrocytes) whose activation may modulate GABA release from MF terminals. It is known that early in postnatal life GABA can be released in a calcium- and SNARE-independent way by non-conventional release sites such as growth cones and astrocytes and can diffuse away to activate in a paracrine fashion extrasynaptic receptors³⁵.

What could be the functional role of eCBs-mediated STD-LTD at immature GABAergic MF-CA3 synapses? During postnatal development, activity-dependent changes in synaptic strength are thought to be involved in the refinement of neuronal circuits³⁶. At early developmental stages eCBs are known to be present, especially in brain areas that control movements, cognition and attention as well as emotion and memory^{37–39}. During gestation, CB1 receptors are enriched in axonal growth cones of cortical GABAergic interneurons where they contribute to regulate axonal guidance, selective targeting and synaptogenesis⁴⁰. During postnatal development, changes in CB1 receptor expression may underlie the age-dependent magnitude of eCB-mediated i-LTD an effect that parallels the sensitivity of GABAergic⁴¹ and glutamatergic⁴² neurotransmission to eCBs. Also at Schaffer collateral-CA1 synapses, the heterosynaptic eCB-mediated persistent depression of glutamate release observed immediately after birth disappears in the mature hippocampus²⁰. Our data suggest that in early postnatal life, eCBs counter the excitatory actions of glutamate and GABA, thus preventing at the network level neuronal hyperexcitability.

Methods

Slice preparation. All experiments were carried out in accordance with the European Community Council Directive of 24 November 1986 (86/609EEC) and were approved by local veterinary authorities (Dr. Giuseppe Stradaoli). All efforts were made to minimize animal suffering and to reduce the number of animal used. Experiments were performed on hippocampal slices from P3–P6 and P19–P25 old Wistar rats, and from *CB1*-KO mice and WT littermate⁴³ of the same postnatal age, following a method already described by Gasparini *et al.*⁴⁴. Briefly, animals were decapitated after being anaesthetized with an *i.p.* injection of urethane (2 g/kg). The brain was quickly removed from the skull and placed in ice-cold ACSF containing (in mM): NaCl 130, KCl 3.5, NaH₂PO₄ 1.2, NaHCO₃ 27, MgCl₂ 1.3, CaCl₂ 2, glucose 25, saturated with 95% O₂ and 5% CO₂ (pH 7.3–7.4). Transverse hippocampal slices (400 μm thick) were cut with a vibratome and stored at room temperature (20–24°C) in a holding bath containing the same solution as above. After recovering for at least one hour, single slices were transferred to a recording chamber where they were superfused with oxygenated ACSF at a rate of 2–3 ml/min at 33–35°C.

Electrophysiological recordings. Recordings were made from CA3 pyramidal cells using the whole-cell patch-clamp configuration in current or voltage-clamp mode. Neurons were visualized using an upright microscope (Olympus BX51WI) equipped

with differential interference contrast optics and infrared video camera. Patch electrodes were pulled from borosilicate glass capillaries (Hingelberg, Malsfeld, D). They had a resistance of 4–6 MΩ when filled with an intracellular solution containing (in mM): KCl 140, MgCl₂ 1, HEPES 10, MgATP 4, EGTA 0.5 (pH 7.3). In some experiments, recordings were performed with patch pipettes containing the calcium chelator 1,2-bis (2-aminophenoxy) ethane-N,N,N',N'-tetraacetic acid (BAPTA 20 mM, purchased from Sigma, Milan, Italy). In these cases, the KCl pipette concentration was reduced to 120 mM to maintain osmolarity at ~290 mOsm. Recordings were made with a patch clamp amplifier (Axopatch 1D; Axon Instruments, Foster City, CA). Series resistance was assessed repetitively every five min and in current-clamp recordings compensated at 75% throughout the experiment. Cells exhibiting more than 15–20% changes in series resistance were not analyzed.

GABA_A-mediated synaptic potentials or currents (GSPs or GPSCs) were evoked at 0.05 Hz from a holding potential of –60 mV in the presence of DNQX (50 μM) and D-AP5 (50 μM) to block AMPA- and NMDA-mediated synaptic responses, respectively. We stimulated granule cells minimally in the dentate gyrus^{45,46}. Stimulation intensity was decreased until a single axon may have been activated. We judged that a single fibre terminating on the recorded cell was activated when the mean postsynaptic current amplitude and failure probability remained constant over a range of stimulus intensities near threshold for detecting a response². An abrupt increase in the mean peak amplitude of synaptic currents was observed when the stimulus intensity was further increased. This all or none behaviour and the constant latency and shape of individual synaptic responses over time let us assume that only a single fibre was stimulated. The monosynaptic nature of synaptic currents was supported by unimodal and narrow distributions of latency and rise time which remained constant when the extracellular Ca²⁺/Mg²⁺ concentration ratio was reduced from 2:1.3 to 1:3².

MF inputs were identified on the basis of their sensitivity to the group II and III mGluR agonists 2-amino-4-phosphonobutyric acid (L-AP4), 2S,1'S,2'S)-2-(2'-carboxycyclopropyl)glycine (L-CCG) or dicarboxycyclopropylglycine (DCG-IV), their strong paired pulse facilitation and short-term frequency-dependent facilitation². In neonates, MF-mediated synaptic responses were blocked by bicuculline or picrotoxin, confirming their GABAergic nature. In contrast to MF inputs, GABAergic inputs from interneurons were insensitive to mGluR agonists^{23,33}.

STD-LTD was induced in current clamp mode by pairing postsynaptic spikes with MF stimulation. MF-GPSCs were recorded first in voltage clamp mode for 5–10 min to obtain a stable baseline. Then a sequence of postsynaptic spike-MF stimulation was repeated ten times at 0.1 Hz with a delay of 50 ms (in some cases also with a delay of 100 and 200 ms) between postsynaptic spiking and presynaptic MF stimulation. Changes in synaptic efficacy were monitored by recording synaptic currents for additional 20–30 min after pairing.

In some experiments, antidromic action potentials were recorded from visually identified granule cells in dentate gyrus. In this case the intracellular solution contained K-gluconate (150 mM) instead of KCl. Extracellular stimuli (at 0.3 Hz, duration 150 μs) were delivered *via* a stimulation electrode positioned in stratum lucidum ~200 μm away from the granule cell layer.

Drugs used were: N-(Piperidin-1-yl)-5-(4-iodophenyl)-1-(2,4-dichlorophenyl)-4-methyl-1H-pyrazole-3-carboxamide (AM251), N-(4-Hydroxyphenyl)-5Z,8Z,11Z,14Z-eicosatetraenamide (AM404), N-(2-Hydroxyethyl)-5Z,8Z,11Z,14Z-eicosatetraenamide (Anandamide, AEA), atropine, 3-[[[(3,4-dichlorophenyl)methyl]amino]propyl]diethoxymethylphosphinic acid (CGP 52432), D-(-)-2-amino-5-phosphopentanoic acid (D-AP5), dihydro-β-erythroidine (DHβE), 6,7-dinitroquinoxaline-2,3-dione (DNQX), 8-Cyclopentyl-1,3-dipropylxanthine (DPCPX), L-(+)-2-amino-4-phosphonobutyric acid (L-AP4), dicarboxycyclopropylglycine (DCG-IV), 2S,1'S,2'S)-2-(2'-carboxycyclopropyl)glycine (L-CCG), (2S)-2-amino-2-[(1S,2S)-2-carboxycycloprop-1-yl]-3-(xanth-9-yl)propanoic acid (LY367385), 2-Methyl-6-(phenylethynyl)pyridine hydrochloride (MPEP), nifedipine, picrotoxin (PTX), tetrahydrolipstatin (THL), R-(+)-[2,3-Dihydro-5-methyl-3-(4-orphenolylmethyl)pyrrolo[1,2,3-de]-1,4-benzoxazin-6-yl]-1-naphthalenylmethanone mesylate (WIN 55,212-2 mesylate), (all purchased from Tocris Cookson Ltd, Bristol, UK); 4-[[4-formyl-5-hydroxy-6-methyl-3-[(phosphonoxy)methyl]-2pyridinyl]azo]-1,3-benzenedisulfonic acid tetrasodium salt (PPADS), (from Sigma, Milan, Italy); 4-nitrophenyl-4-(dibenzo[d][1,3]dioxol-5-yl)(hydroxy)methylpiperidine-1-carboxylate (JZL 184), (3'-(aminocarbonyl)[1,1'-biphenyl]-3-yl)-cyclohexylcarbamate (URB597) from Cayman Chemicals. All drugs were dissolved in either distilled water or ethanol, as required, except DNQX, WIN 55,212-2 mesylate, AM251 and URB597 which were dissolved in dimethylsulphoxide (DMSO). The final concentration of DMSO in the bathing solution was 0.1%. At this concentration, DMSO alone did not modify the shape or the kinetics of synaptic currents. Drugs were applied by changing the bath superfusion solution *via* a three-way tap system. Complete exchange was obtained within 1–2 min.

Data acquisition and analysis. Data were acquired and digitized with an A/D converter (Digidata 1200, Molecular Devices) and stored on a computer hard disk. Acquisition and analysis of evoked responses were performed with Clampfit 9 (Molecular Devices). Data were sampled at 20 kHz and filtered with a cut off frequency of 1 kHz. Mean GPSCs amplitude was obtained by averaging successes and failures. The paired pulse ratio (PPR) was calculated as the mean amplitude of the synaptic response evoked by the second stimulus over that evoked by the first one. The coefficient of variation was calculated as the ratio of the standard deviation and the mean synaptic current amplitude. Unless otherwise stated, data are presented as



mean \pm SEM. Statistical analysis was done using either Student's paired *t*-test for single comparisons or one-way ANOVA for multiple comparisons. A *p* value $<$ 0.05 was considered statistically significant.

Fluorescent in situ hybridization (ISH). The brains of P3 and P21 null CB1 mutant mice and wild-type littermates were isolated, quickly frozen on dry ice and stored at -80° C until sectioning in a cryostat (14 μ m, Microm HM 500 M, Microm Microtech, France). A DIG-labelled riboprobe against mouse CB1 receptor was used²¹ and procedures were as previously described using the TSA amplification System⁴⁷. Slides were analyzed by epifluorescence microscopy at 20X (Leica) and photographed using a Coolsnap HQ2 camera (Roper). In order to detect low but specific levels of labelling, the acquisition parameters were chosen using CB1-KO sections in order to exclude any background signal and exactly the same parameters were immediately used to acquire the images from wild-type P3 and P21 sections. Images of CB1 mRNA labelling did not undergo any post-acquisition processing.

Images of CB1 mRNA FISH were acquired in epifluorescence and the levels of expression were evaluated using the program Image J on 4–8 sections corresponding to dorsal DG of wild-type and CB1-KO P3 and P21 mice (2 mice per group). The levels of fluorescent signal were measured by pixel intensity in black and white images after background subtraction for each section (same parameters for all samples). Six regions of interest were randomly chosen for each section corresponding to the granule cell layer of the dentate gyrus, with the only limit to avoid brightly stained cells, presumably corresponding to GABAergic interneurons²¹. The average values of each section represented one data point. Values were also obtained in a similar way from P3 and P21 CB1-KO mice.

- Henze, D. A., Urban, N. N. & Barrionuevo, G. The multifarious hippocampal mossy fiber pathway: a review. *Neuroscience* **98**, 407–427 (2000).
- Safulina, V. F., Fattorini, G., Conti, F. & Cherubini, E. Gabaergic Signaling At Mossy Fiber Synapses In Neonatal Rat Hippocampus. *J. Neurosci.* **26**, 597–608 (2006).
- Safulina, V. F. *et al.* Control of GABA release at single mossy fiber-CA3 connections in the developing hippocampus. *Front Syn Neurosci* **2**, 1–11. doi:10.3389/neuro.19.003 (2010).
- Safulina, V. F. & Cherubini, E. At immature mossy fibers-CA3 connections, activation of presynaptic GABA_B receptors by endogenously released GABA contributes to synapses silencing. *Front. Neurosci.* **3**, 1–11 (2009).
- Caiati, M. D., Sivakumaran, S. & Cherubini, E. In the developing rat hippocampus, endogenous activation of presynaptic kainate receptors reduces GABA release from mossy fiber terminals. *J. Neurosci.* **30**, 1750–1759 (2010).
- Kasyanov, A. M., Safulina, V. F., Voronin, L. L. & Cherubini, E. GABA-mediated giant depolarizing potentials as coincidence detectors for enhancing synaptic efficacy in the developing hippocampus. *Proc. Natl. Acad. Sci. U S A* **101**, 3967–3972 (2004).
- Sivakumaran, S., Mohajerani, M. H. & Cherubini, E. At immature mossy fiber-CA3 synapses correlated pre and postsynaptic activity persistently enhances GABA release and network excitability via BDNF and cAMP-dependent PKA. *J. Neurosci.* **29**, 2637–2647 (2009).
- Kano, M., Ohno-Shosaku, T., Hashimoto-dani, Y., Uchigashima, M. & Watanabe, M. Endocannabinoid-mediated control of synaptic transmission. *Physiol. Rev.* **89**, 309–380 (2009).
- Heifets, B. D. & Castillo, P. E. Endocannabinoid signaling and long-term synaptic plasticity. *Annu. Rev. Physiol.* **71**, 283–306 (2009).
- Faber, D. S. & Korn, H. Applicability of the coefficient of variation method for analyzing synaptic plasticity. *Biophys. J.* **60**, 1288–1294 (1991).
- Chevalleyre, V. & Castillo, P. E. Heterosynaptic LTD of hippocampal GABAergic synapses: a novel role of endocannabinoids in regulating excitability. *Neuron* **8**, 461–472 (2003).
- Sjöström, P. J., Turrigiano, G. G. & Nelson, S. B. Neocortical LTD via coincident activation of presynaptic NMDA and cannabinoid receptors. *Neuron* **39**, 641–654 (2003).
- Ronesi, J., Gerdeman, G. L. & Lovinger, D. M. Disruption of endocannabinoid release and striatal long-term depression by postsynaptic blockade of endocannabinoid membrane transport. *J. Neurosci.* **24**, 1673–1679 (2004).
- Lourenço, J. *et al.* Synaptic activation of kainate receptors gates presynaptic CB1 signaling at GABAergic synapses. *Nat. Neurosci.* **13**, 197–204 (2010).
- Bisogno, T. *et al.* Cloning of the first sn1-DAG lipases points to the spatial and temporal regulation of endocannabinoid signaling in the brain. *J. Cell Biol.* **163**, 463–468 (2003).
- Katona, I. *et al.* Molecular composition of the endocannabinoid system at glutamatergic synapses. *J. Neurosci.* **26**, 5628–5637 (2006).
- Piomelli, D. The molecular logic of endocannabinoid signalling. *Nat. Rev. Neurosci.* **4**, 873–884 (2003).
- Zucker, R. S. & Regehr, W. G. Short-term synaptic plasticity. *Annu. Rev. Physiol.* **64**, 355–405 (2002).
- Németh, B., Ledent, C., Freund, T. F. & Hájos, N. CB1 receptor-dependent and -independent inhibition of excitatory postsynaptic currents in the hippocampus by WIN 55,212-2. *Neuropharmacology* **54**, 51–57 (2008).
- Yasuda, H., Huang, Y. & Tsumoto, T. Regulation of excitability and plasticity by endocannabinoids and PKA in developing hippocampus. *Proc. Natl. Acad. Sci. U S A* **105**, 3106–3111 (2008).
- Marsicano, G. & Lutz, B. Expression of the cannabinoid receptor CB1 in distinct neuronal subpopulations in the adult mouse forebrain. *Eur. J. Neurosci.* **11**, 4213–4225 (1999).
- Hofmann, M. E., Nahir, B. & Frazier, C. J. Excitatory afferents to CA3 pyramidal cells display differential sensitivity to CB1 dependent inhibition of synaptic transmission. *Neuropharmacology* **55**, 1140–1146 (2008).
- Astori, S., Pawlak, V. & Köhr, G. Spike-timing-dependent plasticity in hippocampal CA3 neurons. *J. Physiol.* **588**, 4475–4488 (2010).
- Di Marzo, V. *et al.* Formation and inactivation of endogenous cannabinoid anandamide in central neurons. *Nature* **372**, 686–691 (1994).
- Kreitzer, A. C. & Regehr, W. G. Retrograde inhibition of presynaptic calcium influx by endogenous cannabinoids at excitatory synapses onto Purkinje cells. *Neuron* **29**, 717–727 (2001).
- Choi, S. & Lovinger, D. M. Decreased frequency but not amplitude of quantal synaptic responses associated with expression of corticostriatal long-term depression. *J. Neurosci.* **17**, 8613–8620 (1997).
- Gerdeman, G. L., Ronesi, J. & Lovinger, D. M. Postsynaptic endocannabinoid release is critical to long-term depression in the striatum. *Nat. Neurosci.* **5**, 446–451 (2002).
- Di Marzo, V. & De Petrocellis, L. Endocannabinoids as regulators of transient receptor potential (TRP) channels: A further opportunity to develop new endocannabinoid-based therapeutic drugs. *Curr. Med. Chem.* **17**, 1430–1449 (2010).
- Azad, S. C. *et al.* Circuitry for associative plasticity in the amygdala involves endocannabinoid signaling. *J. Neurosci.* **24**, 9953–9961 (2004).
- Beltramo, M. *et al.* Functional role of high-affinity anandamide transport, as revealed by selective inhibition. *Science* **277**, 1094–1097 (1997).
- Mor, M. *et al.* Cyclohexylcarbamic acid 3'- or 4'-substituted biphenyl-3-yl esters as fatty acid amide hydrolase inhibitors: Synthesis, quantitative structureactivity relationships, and molecular modeling studies. *J. Med. Chem.* **47**, 4998–5008 (2004).
- Gobbi, G. *et al.* Antidepressant-like activity and modulation of brain monoaminergic transmission by blockade of anandamide hydrolysis. *Proc. Natl. Acad. Sci. U S A* **102**, 18620–18625 (2005).
- Walker, M. C., Ruiz, A. & Kullmann, D. M. Monosynaptic GABAergic signaling from dentate to CA3 with a pharmacological and physiological profile typical of mossy fiber synapses. *Neuron* **29**, 703–715 (2001).
- Dupuy, S. T. & Houser, C. R. Developmental changes in GABA neurons of the rat dentate gyrus: an in situ hybridization and birth dating study. *J. Comp. Neurol.* **389**, 402–418 (1997).
- Demarque, M. *et al.* Paracrine intercellular communication by a Ca²⁺- and SNARE-independent release of GABA and glutamate prior to synapse formation. *Neuron* **36**, 1051–1061 (2002).
- Mohajerani, M. H., Sivakumaran, S., Zacchi, P., Aguilera, P. & Cherubini, E. Correlated network activity enhances synaptic efficacy via BDNF and the ERK pathway at immature CA3-CA1 connections in the hippocampus. *Proc. Natl. Acad. Sci. USA* **104**, 13176–13181 (2007).
- Fernández-Ruiz, J., Berrendero, F., Hernández, M. L. & Ramos, J. A. The endogenous cannabinoid system and brain development. *Trends Neurosci* **23**, 14–20 (2000).
- Wang, X., Dow-Edwards, D., Keller, E. & Hurd, Y. L. Preferential limbic expression of the cannabinoid receptor mRNA in the human fetal brain. *Neuroscience* **118**, 681–694 (2003).
- Zurolo, E. *et al.* CB1 and CB2 cannabinoid receptor expression during development and in epileptogenic developmental pathologies. *Neuroscience* **170**, 28–41 (2010).
- Berghuis, P. *et al.* Hardwiring the brain: endocannabinoids shape neuronal connectivity. *Science* **316**, 1212–1216 (2007).
- Kang-Park, M. H., Wilson, W. A., Kuhn, C. M., Moore, S. D. & Swartzwelder, H. S. Differential sensitivity of GABA A receptor-mediated IPSCs to cannabinoids in hippocampal slices from adolescent and adult rats. *J. Neurophysiol.* **98**, 1223–1230 (2007).
- Al-Hayani, A. & Davies, S. N. Cannabinoid receptor mediated inhibition of excitatory synaptic transmission in the rat hippocampal slice is developmentally regulated. *Br. J. Pharmacol.* **131**, 663–665 (2000).
- Marsicano, G. *et al.* The endogenous cannabinoid system controls extinction of aversive memories. *Nature* **418**, 530–534 (2002).
- Gasparini, S., Saviane, C., Voronin, L. L. & Cherubini, E. Silent synapses in the developing hippocampus: lack of functional AMPA receptors or low probability of glutamate release? *Proc. Natl. Acad. Sci. U S A* **97**, 9741–9746 (2000).
- Jonas, P., Major, G. & Sakmann, B. Quantal components of unitary EPSCs at the mossy fiber synapse on CA3 pyramidal cells of rat hippocampus. *J. Physiol.* **472**, 615–663 (1993).2005).
- Allen, C. & Stevens, C. F. An evaluation of causes for unreliability of synaptic transmission. *Proc. Natl. Acad. Sci. U S A* **91**, 10380–10383 (1994).
- Bellocchio, L. *et al.* Bimodal control of stimulated food intake by the endocannabinoid system. *Nat Neurosci* **13**, 281–283 (2010).

Acknowledgements

This work was supported by a grant from Ministero Istruzione Università e Ricerca (Grant MIUR-PRIN 2009).



Author contributions

MDC, SS, GM, CM, RM, EC designed the study and planned the experiments; MDC, SS, FL, GM, ER and DV performed experiments and analyzed data; EC prepared the manuscript with the help of the other authors.

Additional information

Supplementary information accompanies this paper at <http://www.nature.com/scientificreports>

Competing financial interests: The authors declare no competing financial interests.

License: This work is licensed under a Creative Commons Attribution-NonCommercial-ShareAlike 3.0 Unported License. To view a copy of this license, visit <http://creativecommons.org/licenses/by-nc-sa/3.0/>

How to cite this article: Caiati, M.D. *et al.* Developmental regulation of CB1-mediated spike-time dependent depression at immature mossy fiber-CA3 synapses. *Sci. Rep.* **2**, 285; DOI:10.1038/srep00285 (2012).